

# Disruption of the Disulfide Bonds of Recombinant Murine Interleukin-6 Induces Formation of a Partially Unfolded State<sup>†</sup>

Jian-Guo Zhang,<sup>‡</sup> Jacqueline M. Matthews,<sup>‡</sup> Larry D. Ward,<sup>‡</sup> and Richard J. Simpson\*

Joint Protein Structure Laboratory, Ludwig Institute for Cancer Research and Walter and Eliza Hall Institute of Medical Research, Parkville, Victoria 3050, Australia

Received August 27, 1996; Revised Manuscript Received December 24, 1996<sup>®</sup>

**ABSTRACT:** A chemical modification approach was used to investigate the role of the two disulfide bonds of recombinant murine interleukin-6 (mIL-6) in terms of biological activity and conformational stability. Disruption of the disulfide bonds of mIL-6 by treatment with iodoacetic acid (IAA-IL-6) or iodoacetamide (IAM-IL-6) reduced the biological activity, in the murine hybridoma growth factor assay, by 500- and 200-fold, respectively. Both alkylated derivatives as well as the fully reduced (but not modified) molecule (DTT-IL-6) retained a high degree of  $\alpha$ -helical structure as measured by far-UV CD (37–51%) when compared to the mIL-6 (59%). However, the intensity of the near-UV CD signal of the S-alkylated derivatives was very low relative to that of mIL-6, suggesting a reduction in fixed tertiary interactions. Both IAA-IL-6 and IAM-IL-6 exhibit native-like unfolding properties at pH 4.0, characteristic of a two-state unfolding mechanism, and are destabilized relative to mIL-6, by  $0.3 \pm 1.6$  and  $2.4 \pm 1.2$  kcal/mol, respectively. At pH 7.4, however, both modified proteins display stable unfolding intermediates. These intermediates are stable over a wide range of GdnHCl concentrations (0.5–2 M) and are characterized by increased fluorescence quantum yield and a blue shift of  $\lambda_{\text{max}}$  from 345 nm, for wild-type recombinant mIL-6, to 335 nm. These properties were identical to those observed for DTT-IL-6 in the absence of denaturant. DTT-IL-6 appears to form a partially unfolded and highly aggregated conformation under all conditions studied, as showed by a high propensity to self-associate (demonstrated using a biosensor employing surface plasmon resonance), and an increased ability to bind the hydrophobic probe 8-anilino-1-naphthalenesulfonic acid. The observed protein concentration dependence of the fluorescence characteristics of these mIL-6 derivatives is consistent with the aggregation of partially folded forms of DTT-IL-6, IAM-IL-6, and IAA-IL-6 during denaturant-induced unfolding. For all forms of the protein studied here, the aggregated intermediates unfold at similar denaturant concentrations (2.1–2.9 M GdnHCl), suggesting that the  $\alpha$ -helical structure and nonspecific hydrophobic interprotein interactions are of similar strength in all cases.

Interleukin-6 (IL-6)<sup>1</sup> is a pleiotropic cytokine that plays a central role in host defense mechanisms against infection and tissue injury (Akira et al., 1993; Narazaki & Kishimoto, 1994). Dysregulated production of IL-6 is implicated in the pathology of many disease states, including multiple myeloma (Klein et al., 1995), rheumatoid arthritis, AIDS, psoriasis, Kaposi's sarcoma, and osteoporosis (Hirano, 1994). Recently, a variant of human interleukin-6 (hIL-6) which lacks the 22 N-terminal residues and one of two disulfide

bonds by the double mutation of Cys44 and Cys50 to serine (Breton et al., 1995) has been shown to have a stable molten globule conformation at low pH (De Filippis et al., 1996).

The molten globule of protein folding was originally proposed as a partially folded state with a molecular volume between that of the folded and unfolded states, possessing a high degree of secondary structure but no fixed tertiary interactions (Ptitsyn, 1987). The term is now used to describe more loosely defined collapsed states with little, rather than no tertiary structure. Molten globules have been proposed to be common intermediates on the kinetic folding pathways of all proteins [reviewed by Ptitsyn (1992)], can be bound by molecular chaperones (Flynn et al., 1993; Hayer-Hartl et al., 1994), and may be involved in physiological processes and genetic diseases (Ptitsyn, 1995; Thomas et al., 1995). Stable molten globule states have been studied under conditions of extreme pH and ionic strength (Goto & Fink, 1989), low levels of denaturant (Hagihara et al., 1993; Kreimer et al., 1994), high pressure (Peng et al., 1994), the presence of organic solvent (Wicar et al., 1994) and by the modification of disulfide bonds (Creighton & Ewbank, 1994). The most commonly characterized molten globules are those formed under acidic conditions, which are additionally referred to as the "A-states" (Kuwajima, 1989). The A-state of the single disulfide variant of hIL-6

<sup>†</sup>Supported by Grant 920528 from the National Health and Medical Research Council, Australia.

\* Address correspondence to Dr. Richard J. Simpson, Ludwig Institute for Cancer Research and the Walter and Eliza Hall Institute of Medical Research, PO Royal Melbourne Hospital, Parkville, Victoria 3050, Australia. Fax: +61 3 9348 1925. Telephone: +61 3 9347 3155. E-mail: simpson@licre.ludwig.edu.au.

<sup>‡</sup>These authors contributed equally to this work.

<sup>®</sup> Abstract published in *Advance ACS Abstracts*, February 1, 1997.

<sup>1</sup> Abbreviations: ANS, 8-anilino-1-naphthalenesulfonic acid; CD, circular dichroism; DTT, dithiothreitol; DTT-IL-6, fully reduced recombinant murine interleukin-6; G-CSF, granulocyte colony-stimulating factor; GdnHCl, guanidinium hydrochloride; hIL-6, recombinant human interleukin-6; IAA, iodoacetic acid; IAA-IL-6, fully reduced and S-carboxymethylated recombinant murine interleukin-6; IAM, iodoacetamide; IAM-IL-6, fully reduced and S-carbamidomethylated recombinant murine interleukin-6; IL-6, interleukin-6; IL-6R, interleukin-6 receptor; mIL-6, recombinant murine interleukin-6; RP-HPLC, reversed-phase high-performance liquid chromatography; SEC, size-exclusion chromatography; SPR, surface plasmon resonance.

has recently been reported to be protease resistant (De Filippis et al., 1996). A molten globule conformation may thus be advantageous in maintaining the IL-6 activity evident at inflammation sites (De Filippis et al., 1996), which are characterized by low pH and an increased level of proteases (Silver et al., 1988).

Murine IL-6 (mIL-6) has a 42% amino acid sequence identity and a selective cross reactivity with hIL-6, whereby hIL-6 is active on mouse cells, but not *vice versa*. In order to determine the cause of aggregation of mIL-6 at high protein concentrations (Morton et al., 1995), we have studied the equilibrium denaturant-induced unfolding of mIL-6 (Ward et al., 1995; Matthews et al., 1996). At pH 7.4, or at pH 4.0 in the presence of salt, unfolding intermediates, which are proposed to be molten globule-like, accumulate. In contrast, at pH 4.0, under low salt conditions, the urea-induced unfolding of mIL-6 is apparently two-state (Ward et al., 1995).

To establish the nature of the mIL-6 equilibrium unfolding intermediates, to compare their properties with those of the hIL-6 molten globule, and to determine the role of the two disulfide bonds in its biological activity and conformational stability, we have investigated the folding and conformational properties of mIL-6 upon reduction and chemical modification of its cysteine residues. In this paper, we characterize these reduced and cysteine-modified forms of mIL-6 in terms of their spectral and unfolding properties. S-alkylation of the four cysteine residues of mIL-6 with either iodoacetic acid or iodoacetamide induces a partially folded conformation of the molecule with high secondary but low tertiary structure. Upon exposure to denaturant or at high protein concentrations, these conformations have a high tendency to aggregate and are shown to resemble those observed in denaturant-induced unfolding of wild-type recombinant mIL-6. The properties of these intermediate folded forms are discussed in terms of previously described, stable, partially folded forms characterized in other protein systems, including the above-mentioned molten globule state.

## MATERIALS AND METHODS

**Preparation of S-Alkylated Forms of Murine IL-6.** Recombinant mIL-6 was expressed in *Escherichia coli* (Simpson et al., 1988a) and purified to homogeneity as described previously (Zhang et al., 1992). The first eight residues of mIL-6 are derived from the N terminus of bacterial  $\beta$ -galactosidase and the polylinker region of pUC9, while the remaining 176 amino acids correspond to residues 12–187 of natural mIL-6 (Simpson et al., 1988b). Lyophilized mIL-6 (0.5 mg/mL) was dissolved in 0.1 M Tris-HCl (pH 8.3), 1 mM EDTA, 6 M GdnHCl (Pierce), and 5 mM dithiothreitol (DTT, Sigma) and incubated for 2 h at 22 °C to fully reduce the disulfide bonds. Fully reduced mIL-6 (DTT-IL-6) was then treated with either 20 mM iodoacetic acid (IAA, Fluka) or 20 mM iodoacetamide (IAM, Fluka) for 40 min at 22 °C in the dark, and the alkylation reactions were quenched by the addition of excess  $\beta$ -mercaptoethanol. The alkylated proteins were desalted and purified using a Vydac C4 (10 mm  $\times$  100 mm) RP-HPLC system using a linear acetonitrile/trifluoroacetic acid gradient (Zhang et al., 1992) and lyophilized. The resultant powders were readily dissolved in water and subsequently diluted into the appropriate buffers for spectrophotometric analysis.

**Biological Assays.** The hybridoma growth factor assay was performed as described by van Snick et al. (1986). Briefly, IL-6-dependent murine hybridoma 7TD1 cells were incubated in a 96-well microtiter plate (2000 cells/microwell), with serial dilutions of the test samples in a total volume of 0.2 mL. Cell numbers were evaluated after 4 days at 37 °C by measuring hexosaminidase levels (Landegren, 1984). Competitive receptor binding assays were performed using 7TD1 cells as described previously (Ward et al., 1993).

**Estimation of Protein Concentration.** Protein concentrations were determined by amino acid analysis using a Beckman amino acid analyzer (model 6300) equipped with a model 7000 data system (Simpson et al., 1986). Samples were hydrolyzed *in vacuo* at 110 °C for 16 h with 6 M HCl containing 0.1% (w/v) phenol.

**Spectroscopic Measurements.** Circular dichroism measurements were performed at 25 °C using an Aviv Model 62DS (Lakewood, NJ) CD spectrometer. Far-UV CD spectra were recorded using a 0.1 cm path length cell and protein concentrations of 50–200  $\mu$ g/mL (as indicated in the text). Near-UV CD spectra were recorded using a concentration of 1 mg/mL and a 1 cm path length cell. Reported spectra are expressed in terms of mean residue ellipticity  $[\Theta]_{MRW}$  which were calculated using a mean residue weight of 115.5. All solutions were filtered with 0.22  $\mu$ m pore size filters (Millipore) prior to recording spectra. Data were collected using an averaging time of 1 s, a step size of 0.2 nm, and a band width of 0.8 nm. Reported spectra are the average of four scans with baseline subtractions. Estimates of  $\alpha$ -helical content were made using the reference spectra of Yang et al. (1986) and a multilinear regression program (Prosec) supplied by Aviv. Denaturation experiments were monitored at 222 nm. Fluorescence data were collected on a Perkin-Elmer model LS5 luminescence spectrophotometer using 0.5 cm path length cells at 25 °C and a 5 nm emission slit width. Excitation wavelengths were 295 nm for tryptophan fluorescence and 350 nm for ANS fluorescence.

**8-Anilino-1-naphthalenesulfonic Acid Binding.** The interaction of ANS (Molecular Probes) with mIL-6 and its cysteine-modified derivatives was monitored by measuring the change in the fluorescence emission spectrum of ANS ( $2.5 \times 10^{-6}$  M) in the presence of the respective protein (50  $\mu$ g/mL).

**Denaturant-Induced Unfolding.** Urea- and GdnHCl-induced unfolding of mIL-6 and the alkylated derivatives were monitored by (i) the changes in the CD signal at 222 nm, (ii) the intrinsic fluorescence (emission intensity at 335 nm), and (iii) the intrinsic fluorescence  $\lambda_{max}$  in the range of 310–400 nm as a function of denaturant concentration, and the extrinsic fluorescence by monitoring the change of ANS fluorescence (emission intensity at 472 nm, and  $\lambda_{max}$  in the range of 410–590 nm) in either 10 mM Tris-HCl at pH 7.4 or 10 mM sodium acetate at pH 4.0 (Ward et al., 1995). Solutions were incubated at 25 °C for at least 2 h prior to measurement. Where appropriate, data were analyzed using eq 1 [based on eq 4 in Santoro and Bolen (1988) and eq 11 in Clarke and Fersht (1993)], assuming a two-state unfolding transition with pre- and post-transition dependence of baselines on denaturant concentration, to yield estimates of  $[D]_{50\%}$ , the denaturant concentration at the midpoint of unfolding,  $m$ , the slope of the unfolding curve in the transition region, and  $\Delta G_{unf}$ , the free energy of unfolding extrapolated to water.

$$S = \frac{S_N - a[D] + (S_U - b[D]) \exp(A)}{1 + \exp(A)} \quad (1)$$

where,  $A = (m[D] - \Delta G_{\text{unf}})/RT = m([D] - [D]_{50\%})/RT$ .  $S$  is the measured property of the protein at a given denaturant ( $D$ ) concentration.  $S_N$  is the signal of the native state.  $S_U$  is the signal of the unfolded state.  $R$  is the gas constant, and  $T$  is the absolute temperature.  $a$  and  $b$  are the slopes of the pre- and post-transitional baselines, respectively. Data were fitted using the nonlinear regression analysis program Kaleidagraph (version 3.0, Synergy Software; PCS Inc.).

**Monitoring of mIL-6 Self-Association.** The self-association of mIL-6 and DTT-IL-6 was monitored by surface plasmon resonance (SPR) using a BIAcore instrument (Pharmacia, Sweden). mIL-6 was covalently attached to the carboxylated dextran matrix of the gold biosensor chip using *N*-ethyl-*N'*-[3-(diethylamino)propyl]carbodiimide/*N*-hydroxysuccinimide coupling chemistry (Ward et al., 1993). The interaction of mIL-6 or DTT-IL-6 with immobilized mIL-6 was monitored at 25 °C in HBS buffer [10 mM HEPES (pH 7.4), 150 mM NaCl, 3.4 mM EDTA, and 0.005% (w/v) Tween-20]. The respective proteins were introduced to the sensor chip surface at a flow rate of 1  $\mu$ L/min for 50 min. Regeneration of the sensor surface between assays was performed by treatment with 6 M GdnHCl for 3 min. We have previously demonstrated that immobilized mIL-6 is stable to multiple regenerations with 6 M GdnHCl (Ward et al., 1993).

**GdnHCl Denaturation Monitored by Size-Exclusion Chromatography.** Size-exclusion chromatography was performed on a 300  $\times$  10 mm Superose-12 column (Pharmacia) using a 1090 Hewlett-Packard liquid chromatograph equipped with an automatic sampler. The column was pre-equilibrated with buffer [10 mM Tris-HCl (pH 7.4) and 100 mM NaCl] containing the appropriate concentration of GdnHCl. Stock solutions of protein in 3 M GdnHCl were kept at 4 °C between runs, and run times were typically 90 min at 0.2 mL/min or 60 min at 0.3 mL/min; the column temperature was  $28 \pm 2$  °C. Elution volumes were taken at the maxima of absorbance peaks detected at 215 nm.

## RESULTS

**Reduction and Alkylation of Murine IL-6.** The two disulfide bonds of mIL-6, Cys44–Cys50<sup>2</sup> and Cys73–Cys83 (Simpson et al., 1988a), were reduced by treatment with DTT prior to alkylation with IAA or IAM. The modified proteins, IAA-IL-6 and IAM-IL-6, appeared as single symmetrical peaks when purified by RP-HPLC (data not shown). Amino acid analysis revealed 4.2 mol of carboxymethylcysteine per mole of IAA-IL-6 and 4.1 mol of carbamidomethylcysteine per mole of IAM-IL-6 (data not shown). The molar ratios of the other amino acids were in excellent agreement with those predicted for wild-type recombinant mIL-6. These data indicated that the S-alkylation reaction had gone to completion and that no discernible side reactions of the alkylating reagents with other potentially reactive amino acid residues such as methionine, histidine, and lysine (Glazer et al., 1975) had occurred.

**Biological Properties of IAA-IL-6 and IAM-IL-6.** In comparison with wild-type recombinant mIL-6, both alky-

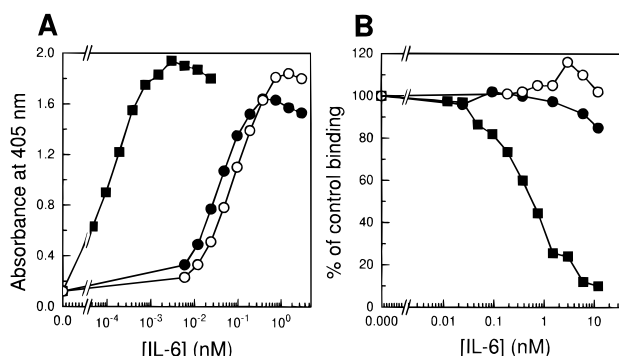


FIGURE 1: Effect of reduction and alkylation on biological activity and receptor-binding capacity of mIL-6: IAA-IL-6 (●), IAM-IL-6 (○), and mIL-6 (■). (A) Hybridoma 7TD1 growth factor activity. (B) Receptor binding capacity. The binding is expressed as a relative value where the binding obtained without competitors is taken as 100%.

lated forms of mIL-6 showed a 200–500-fold decrease in potency in the murine hybridoma 7TD1 growth factor assay (Figure 1A). The specific activities of IAM-IL-6 and IAA-IL-6 were  $5.7 \times 10^5$  and  $1.3 \times 10^6$  u/mg, respectively, compared with  $3.3 \times 10^8$  u/mg for wild-type mIL-6. All control samples (i.e., nonreduced mIL-6 treated with IAA and IAM and DDT-treated mIL-6 which had not been alkylated) were equipotent with respect to mIL-6 (data not shown). During the course of the 7TD1 assay, DTT-IL-6 re-oxidises, readily forming its native disulfide bonds (Zhang et al., 1992), hence its equivalent activity. These data correspond to a decreased ability of IAA-IL-6 and IAM-IL-6 to compete with [<sup>125</sup>I]mIL-6 for binding to 7TD1 cells (Figure 1B), i.e., a decreased binding affinity of the alkylated derivatives for murine IL-6R. While we cannot eliminate the possibility that these biological activities are caused by contaminating amounts (<0.5%) of unmodified mIL-6, the data are consistent with the low levels of activity observed for hIL-6 in which the equivalent disulfide bonds have similarly been reduced and S-alkylated or removed by site-directed mutagenesis (Snouwaert et al., 1991; Rock et al., 1994).

**Conformational Properties as Determined by Fluorescence Spectroscopy.** An excitation wavelength of 295 nm was used to preferentially excite the two tryptophan side chains (Trp34 and Trp157) of mIL-6 (Figure 2). The resultant fluorescence emission spectrum at pH 7.4 is characterized by a  $\lambda_{\text{max}}$  of 347 nm. Lowering the pH to 4.0 quenches the fluorescent yield by  $\approx 40\%$  and causes a small blue-shift of the  $\lambda_{\text{max}}$  to 344 nm. At pH 4.0, the fluorescence spectra of IAA-IL-6 and IAM-IL-6 were similar to that observed for wild-type mIL-6 (Figure 2B). Nearly identical values of  $\lambda_{\text{max}}$  (345 nm) and only small increases of fluorescence emission intensity (IAA-IL-6 < IAM-IL-6) were observed. However, at pH 7.4, larger and more disparate deviations in  $\lambda_{\text{max}}$  were observed (Figure 2A). In particular, IAM-IL-6 shows a  $\lambda_{\text{max}}$  of 341 nm. This significant blue-shift suggests a transfer of the tryptophan side chains in IAM-IL-6 to a more hydrophobic environment, resulting from either conformational changes or protein association. Blue-shifts in  $\lambda_{\text{max}}$  and corresponding increases in quantum yield for mIL-6 have previously been shown to correlate with protein aggregation (Ward et al., 1995). In contrast, large deviations of the fluorescence characteristics were observed for DTT-IL-6 (curve A, Figure 2). The  $\lambda_{\text{max}}$  of DTT-IL-6 underwent a

<sup>2</sup> Using the numbering system for hIL-6 (Simpson et al., 1997).

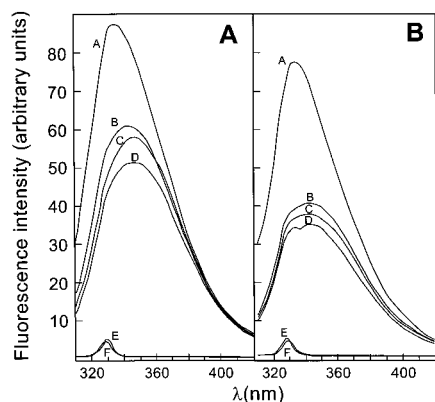


FIGURE 2: Effect of reduction and alkylation of cysteine residues of mIL-6 on intrinsic protein fluorescence. Spectra A–F correspond to DTT-IL-6, IAM-IL-6, IAA-IL-6, mIL-6, buffer, and buffer containing 10 mM DTT, respectively. (A) Spectra were recorded in 10 mM Tris-HCl at pH 7.4. (B) Spectra were recorded in 10 mM sodium acetate at pH 4.0. The protein concentration in all cases was 40  $\mu\text{g/mL}$ . For the preparation of DTT-IL-6, mIL-6 was reduced with 10 mM DTT at room temperature for 5 h at a protein concentration of 400  $\mu\text{g/mL}$  in 10 mM Tris-HCl at pH 7.4 and diluted 10-fold with the appropriate buffer immediately prior to analysis. Samples were incubated at 25  $^{\circ}\text{C}$  for at least 1 h prior to recording the spectra. The spectra of DTT-IL-6 at pH 4.0 or 7.4 were recorded in the presence of 1 mM DTT.

blue shift to 335 nm at both pH 4.0 and 7.4. Concomitantly, the intensity of the fluorescence emission of DTT-IL-6 was dramatically increased by 215 and 170% at pH 4.0 and 7.4, respectively, relative to that of mIL-6, suggesting that DTT-IL-6 is strongly aggregated at both pH values.

**Conformational Properties as Determined by Circular-Dichroism.** While fluorescence yields information on the specific environment of tryptophan side chains, CD reports on the general secondary and tertiary structure of proteins. Far-UV CD gives a measure of the secondary structure of proteins. The far-UV CD spectra of mIL-6 and its alkylated derivatives at both pH 4.0 and 7.4 are shown in Figure 3. IL-6 is a four- $\alpha$ -helix bundle protein (Bazan, 1990; Nishimura et al., 1996), and in all cases, the far-UV CD spectra were characteristic of proteins possessing a high  $\alpha$ -helical content with a maximum at 193 nm and minima at 208 and 222 nm. An inspection of the profiles at pH 7.4 (Figure 3A) revealed that disruption of the disulfide bonds in mIL-6 resulted in conformational differences where the intensity of the CD signal was sensitive to alkylation and the nature of the modifying reagent. The  $\alpha$ -helical contents of these proteins were estimated to be 59, 51, 37, and 43% for mIL-6, IAA-IL-6, IAM-IL-6, and DTT-IL-6, respectively. Only DTT-IL-6 shows a significant change in the shape of its profile at pH 7.4 (Figure 3A). The ratio of CD signals at the two minima characteristic for  $\alpha$ -helices,  $\Theta_{222\text{nm}}/\Theta_{208\text{nm}}$  is typically  $<1$  for coiled-coil structures (Cooper & Woody, 1990), of which a four- $\alpha$ -helix bundle protein is a four-stranded example. Such a ratio is observed for mIL-6 (0.93), IAA-IL-6 (0.87), and IAM-IL-6 (0.98) as expected, while for DTT-IL-6, this ratio is  $>1$  (1.26) which is characteristic of helices in noncoiled peptides (Cooper & Woody, 1990). At pH 4.0, the CD spectra for both alkylated derivatives were similar to that observed for mIL-6 (Figure 3B).

Near-UV CD is an indicator of tertiary structure in proteins, reporting on the environment of aromatic side chains, and the loss of signal in this region is often used to establish molten globule-like properties (Ptitsyn, 1992). The

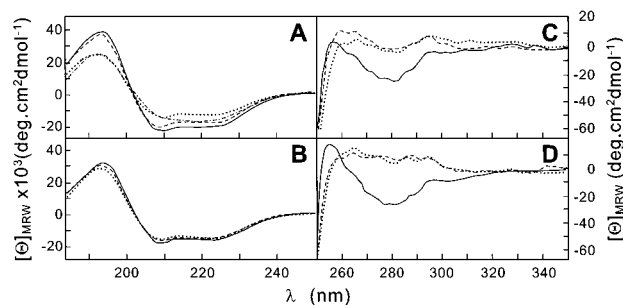


FIGURE 3: Far- and near-UV CD spectra of cysteine-modified derivatives of mIL-6. All spectra were standardized with respect to protein concentration and expressed in terms of mean residue ellipticity  $[\Theta]_{\text{MRW}}$ . Samples were incubated at 25  $^{\circ}\text{C}$  for at least 1 h prior to recording the spectra. Far- and near-UV CD spectra were recorded using 0.1 and 10 cm path length cells, respectively. IAA-IL-6 (—), IAM-IL-6 (···), DTT-IL-6 (— · —), and mIL-6 (—). The protein concentration was 90  $\mu\text{g/mL}$  for IAA-IL-6, IAM-IL-6, and mIL-6 and 45  $\mu\text{g/mL}$  for DTT-IL-6. (A) Far-UV CD spectra at pH 7.4. The buffer was 10 mM sodium phosphate at pH 7.4. For the preparation of DTT-IL-6, mIL-6 was reduced with 10 mM DTT at room temperature for 5 h at a protein concentration of 450  $\mu\text{g/mL}$  in 10 mM Tris-HCl at pH 7.4 and diluted 10-fold with buffer prior to analysis. (B) Far-UV CD spectra at pH 4.0. The buffer was 10 mM sodium acetate at pH 4.0. (C) Near-UV CD spectra at pH 7.4. The buffer was 10 mM Tris-HCl at pH 7.4. (D) Near-UV CD spectra at pH 4.0. The buffer was 10 mM sodium acetate at pH 4.0.

near-UV CD spectra of wild-type mIL-6, IAA-IL-6, and IAM-IL-6 at both pH 7.4 and 4.0 are shown in panels C and D of Figure 3, respectively. The near-UV spectra for DTT-IL-6 are not shown as DTT has a CD signal in this region of the spectrum which obscures the protein signal. The spectra of mIL-6 at pH 7.4 and 4.0 are similar, although the intensities of the CD signal are slightly higher at pH 4.0. Both IAA-IL-6 and IAM-IL-6 show a much reduced signal relative to that of wild-type mIL-6, indicating a significant reduction in tertiary structure. For both IAA-IL-6 and IAM-IL-6 at pH 7.4, the characteristic minimum of mIL-6, at approximately 280 nm, is present but diminished, while at pH 4.0, this minimum is absent.

**ANS Binding.** The fluorescent dye ANS, which undergoes a blue-shift of  $\lambda_{\text{max}}$  and a concomitant increase in fluorescent yield upon exposure to nonpolar environments (such as the binding to clusters of hydrophobic residues in proteins; Dolgikh et al., 1981), was used to probe possible conformational transitions of mIL-6 upon reduction and alkylation. Figure 4 shows the fluorescence emission spectra of ANS ( $2.5 \times 10^{-6}$  M) at pH 4.0 and 7.4, in the presence of 50  $\mu\text{g/mL}$  DTT-IL-6 (a), IAM-IL-6 (b), mIL-6 (c), IAA-IL-6 (d), and buffer only (e). These data show the binding of ANS to all proteins, as indicated by an increase of fluorescence emission intensity and the corresponding blue-shift of  $\lambda_{\text{max}}$ . The extent of binding, however, varies greatly according to the pH and to the type of modification. In all cases, the quantum yield of ANS fluorescence is much higher (8–15-fold) at pH 4.0 than at pH 7.4, with a correspondingly greater blue shift of  $\lambda_{\text{max}}$  [467 to 470 nm at pH 4.0 (Figure 4A) compared with 470 to 499 nm at pH 7.4 (Figure 4B)]. It should be noted that this effect cannot be attributed solely to pH-induced conformational changes of mIL-6. While the fluorescence of mIL-6-bound ANS at pH 4.0 is 8-fold greater than that at pH 7.4, the secondary and tertiary structure of mIL-6 is nearly identical at both pH values (Figure 3) and the protein is essentially monomeric over this pH range,

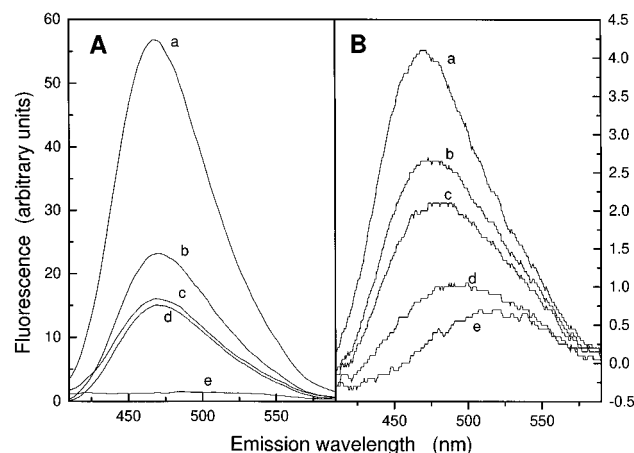


FIGURE 4: Binding of ANS to mIL-6 and its cysteine-modified derivatives: (A) 10 mM sodium acetate at pH 4.0 and (B) 10 mM Tris-HCl at pH 7.4. Spectra are as follows: (a) ANS + DTT-IL-6, (b) ANS + IAM-IL-6, (c) ANS + mIL-6, (d) ANS + IAA-IL-6, and (e) free ANS. The concentration of the proteins was  $50 \mu\text{g/mL}$  in all cases. The ANS concentration was  $2.5 \times 10^{-6}$  M. For the preparation of DTT-IL-6, mIL-6 was reduced with 10 mM DTT at room temperature for 5 h at a protein concentration of  $500 \mu\text{g/mL}$  in 10 mM Tris-HCl at pH 7.4 and diluted 10-fold with buffer prior to analysis. Samples were incubated at  $25^\circ\text{C}$  for 10 min prior to recording the spectra.

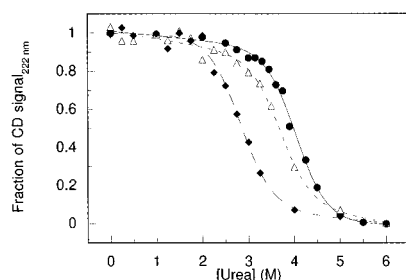


FIGURE 5: Urea-induced equilibrium unfolding of mIL-6 and its alkylated derivatives at pH 4.0, monitored by far-UV CD. The concentration of protein was  $75 \mu\text{g/mL}$  in all cases. The fraction of unfolded protein, calculated on the basis of the relative change in  $[\Theta]_{\text{MRW}}$  at 222 nm, was plotted against the concentration of urea: mIL-6 (●), IAA-IL-6 (△), and IAM-IL-6 (◆). The buffer used was 10 mM sodium acetate at pH 4.0. The data were fitted to eq 1 which assumes a two-state unfolding process.

under low-ionic strength conditions (Ward et al., 1995). DTT-IL-6 has the greatest effect on ANS fluorescence quantum yield, with a 4- and 2-fold increase over that of mIL-6 at pH 4.0 and 7.4, respectively, followed by IAM-IL-6. While at pH 4.0 IAA-IL-6 has an effect on ANS fluorescence similar to that of mIL-6, at pH 7.4, the effect is significantly reduced. In the latter case, the low ANS fluorescence may result from the negatively charged S-modifying groups in IAA-IL-6, which may reduce binding of deprotonated ANS at neutral pH, or may electrostatically quench ANS fluorescence.

**Urea Denaturation and Stability at pH 4.0.** We have previously established that equilibrium unfolding of mIL-6 is very dependent on solution conditions and that apparent two-state unfolding occurs at pH 4.0 when urea is used as the denaturant (Ward et al., 1995). These same conditions were used to determine the relative stabilities of the S-alkylated forms of mIL-6, monitored by the change in the CD signal at 222 nm (Figure 5, Table 1). Monophasic unfolding transitions and the constant  $m$  values suggest that under these conditions the unfolding of the modified forms

Table 1: Values for Urea-Induced Denaturation of Wild-Type Recombinant mIL-6 and S-Carboxymethylated Derivatives at pH 4.0<sup>a</sup>

protein	[urea] <sub>50%</sub> (M)	$m$ (kcal mol <sup>-1</sup> M <sup>-1</sup> )	$\Delta G_{\text{unf}}(\text{H}_2\text{O})$ (kcal mol <sup>-1</sup> )
mIL-6	$4.05 \pm 0.07$	$1.8 \pm 0.2$	$7.2 \pm 0.8$
IAA-IL-6	$3.70 \pm 0.13$	$1.8 \pm 0.4$	$6.7 \pm 1.4$
IAM-IL-6	$2.81 \pm 0.08$	$1.7 \pm 0.3$	$4.8 \pm 0.9$

<sup>a</sup> Data were fitted to eq 1; the tolerances shown are fitting errors.

of mIL-6 remains close to two-state. Whereas IAA-IL-6 is only slightly less stable than mIL-6 ( $-0.3 \pm 1.6$  kcal/mol), IAM-IL-6 is significantly less stable ( $-2.4 \pm 1.2$  kcal/mol).

**Size-Exclusion Chromatography.** Size-exclusion chromatography (SEC) experiments were designed to investigate the hydrodynamic properties of the monomeric unfolding intermediates of mIL-6 and the alkylated proteins (data not shown). We monitored the change in retention volume of the monomer peaks with increasing concentrations of GdnHCl, which was identical for flow rates of 0.2 or 0.3 mL/min. The low observed intensity of the IAA-IL-6 and IAM-IL-6 monomers suggested that aggregation of those stock protein solutions had occurred; however, aggregated forms were not detected in our system, presumably because these very high-molecular weight forms did not enter the gel matrix.

**GdnHCl Denaturation at pH 7.4.** Equilibrium unfolding studies have shown that mIL-6 forms aggregation-prone unfolding intermediates at pH 7.4 when either GdnHCl or urea is used as the denaturant (Ward et al., 1995). The fluorescence properties of DTT-IL-6 (blue-shifted  $\lambda_{\text{max}}$  and an increase of fluorescence quantum yield, Figure 2) closely resemble those of these aggregated, partially unfolded forms of mIL-6. A smaller shift in  $\lambda_{\text{max}}$  and the associated increase of quantum yield for IAA-IL-6 and IAM-IL-6 suggest that there may also be a low level of aggregation of these derivatives. To test whether the addition of low levels of denaturant to the alkylated derivatives would further induce formation of native-like aggregated folding intermediates, GdnHCl-induced unfolding at pH 7.4 was performed (Figure 6). GdnHCl, rather than urea, was used to ensure that the proteins were fully denatured at high denaturant concentrations. Several different methods were used to determine the nature of the potential unfolding intermediates, including (i) SEC to estimate changes in hydrodynamic volume, (ii) far-UV CD at 222 nm to examine the loss of secondary structure, (iii) ANS fluorescence  $\lambda_{\text{max}}$  to monitor the change of the hydrophobic environment (top panels), as well as (iv)  $\lambda_{\text{max}}$  and quantum yield of intrinsic fluorescence to monitor the changing environment of tryptophan residues (bottom panels).

The unfolding of mIL-6 shows several different phases under these conditions (Figure 6A). Following a baseline region (0–1 M GdnHCl), there is a gradual decrease of the retention time (increase of the hydrodynamic volume) from 1 to 1.8 M GdnHCl, accompanied by a blue-shifted ANS and intrinsic  $\lambda_{\text{max}}$  with a concomitant increase of the intrinsic fluorescence quantum yield, and the start of a decrease of the CD signal. This is followed by a major unfolding phase (1.8–3.0 M GdnHCl) with a sharper rate of decrease of the retention time, a red-shift of ANS and intrinsic  $\lambda_{\text{max}}$  with a concomitant loss of intrinsic fluorescence intensity, and a further decrease of the CD signal.

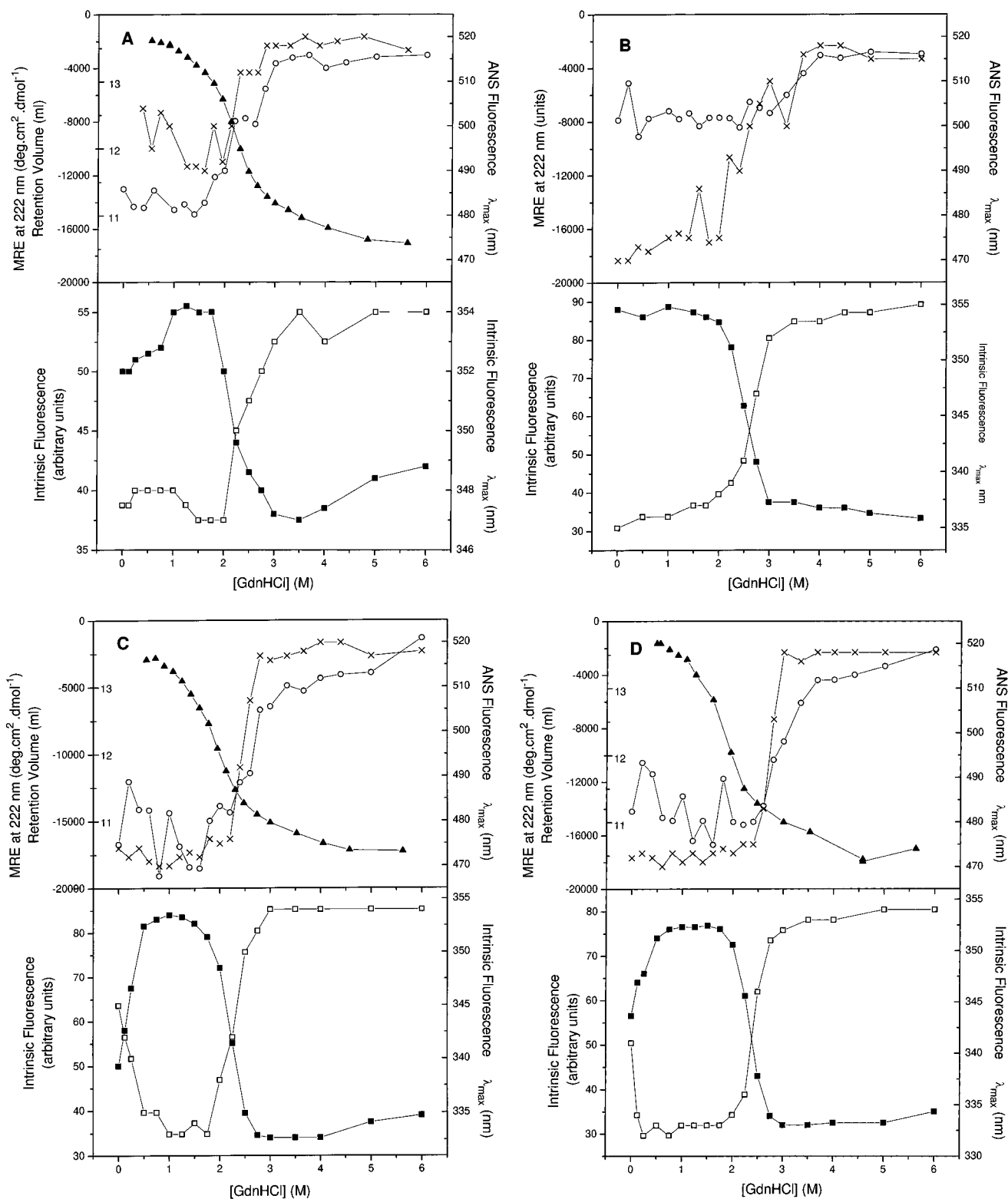


FIGURE 6: GdnHCl-induced equilibrium unfolding of mIL-6 and its cysteine modified derivatives at pH 7.4. In all cases, the fluorescence emission at 335 nm (■), the fluorescence  $\lambda_{\max}$  (□), the MRE of CD signal at 222 nm (O), the retention volume by SEC (▲), and the ANS  $\lambda_{\max}$  (×) were plotted against the concentration of GdnHCl: (A) mIL-6, (B) DTT-IL-6 (no SEC trace is shown for this protein), (C) IAA-IL-6, and (D) IAM-IL-6. The buffer used was 10 mM Tris-HCl at pH 7.4. For intrinsic fluorescence properties, the protein concentration was 40  $\mu\text{g}/\text{mL}$  in all cases. For the CD and ANS binding experiments, the protein concentrations were 70  $\mu\text{g}/\text{mL}$  for mIL-6, IAA-IL-6, and IAM-IL-6 and 60  $\mu\text{g}/\text{mL}$  for DTT-IL-6. All data are shown as line plots and are not fitted to any equation.

The unfolding properties of DTT-IL-6 at pH 7.4 (Figure 6B) are quite different from those of mIL-6. Even in the absence of denaturant, the  $\lambda_{\max}$  of ANS and that of the intrinsic fluorescence are blue-shifted relative to those of mIL-6, while the quantum yield of the intrinsic fluorescence is relatively increased. This is consistent with the fluores-

cence data for DTT-IL-6 at both pH 4.0 and 7.4, where an increased fluorescence signal and low values of  $\lambda_{\max}$  were observed for the native protein (Figure 2). Although there is a gradual red-shift of the  $\lambda_{\max}$  of ANS, the intrinsic fluorescence properties remain constant until 2.0 M GdnHCl, beyond which the protein exhibits a fairly cooperative major

Table 2: Effect of Protein Concentration on Fluorescence  $\lambda_{\max}$  in the Range of 310–400 nm for mIL-6 and IAM-IL-6 at pH 7.4<sup>a</sup>

[protein] ( $\mu\text{g/mL}$ )	$\lambda_{\max}$ (nm)		
	mIL-6	mIL-6 + 1.5 M GdnHCl	IAM-IL-6
40	347	347	341
100	347	344	340
200	347	340	339
300	347	338	337

<sup>a</sup> The excitation wavelength was 295 nm. Buffers were 10 mM Tris-HCl or 10 mM Tris-HCl containing 1.5 M GdnHCl.

unfolding phase. The far-UV CD signal at 222 nm remains constant at 50% of the mIL-6 signal until 3 M GdnHCl, where the loss of the signal coincides with the later half of the unfolding transition detected by the red-shift of ANS binding. There are no SEC data for DTT-IL-6 because of the strong tendencies of this protein to aggregate.

The unfolding of IAA-IL-6 and IAM-IL-6 (panels C and D of Figure 6) under these conditions have some features of both mIL-6 and DTT-IL-6 unfolding. Like those of mIL-6, blue shifted values of intrinsic  $\lambda_{\max}$  with a concomitant increase of the intrinsic fluorescence quantum yield are observed, but these occur at lower, and extend over a larger range of, GdnHCl concentrations (0.5–2.0 M). Like those of DTT-IL-6, values of  $\lambda_{\max}$  of ANS fluorescence are already blue-shifted to 470 nm, with no further increase of the signal with increasing GdnHCl concentrations. The CD signal for these proteins, although scattered, remains fairly constant over this range of GdnHCl concentrations. The major unfolding phases for these proteins, like those of both mIL-6 and DTT-IL-6, begin at 2.0 M GdnHCl, showing relatively sharp red-shifts of ANS  $\lambda_{\max}$  and a change of intrinsic fluorescence properties, but a broad transition region detected by the loss of the far-UV CD signal. For both proteins, and particularly in the case of IAM-IL-6, the major unfolding phase of the monomeric proteins detected by SEC appears to precede that detected by other means, suggesting that aggregation confers an increased stability on the partially unfolded forms of these S-alkylated proteins.

Thus, at pH 7.4, even in the absence of denaturant, DTT-IL-6 appears to have assumed a conformation similar to that of the mIL-6-aggregated unfolding intermediates which accumulate over the GdnHCl concentration range of 1.0–1.8 M at pH 7.4, while IAA-IL-6 and IAM-IL-6 have a tendency to form these unfolding intermediates at lower denaturant concentrations than their parent protein.

The denaturation of the aggregated intermediates of mIL-6 and its S-alkylated derivatives (the major unfolding phase) occurs over a fairly small range of GdnHCl concentrations (2.1–2.4 M as monitored by intrinsic fluorescence and 2.1–2.9 M GdnHCl as detected by far-UV CD and ANS fluorescence; Table 4). DTT-IL-6 appears to unfold at slightly higher denaturant concentrations (2.5–2.7 M urea and 3.4–3.5 M urea, respectively; Table 4).

*Self-Association of the Cysteine-Modified Derivatives of mIL-6.* A blue-shift of fluorescence  $\lambda_{\max}$  (both ANS and intrinsic) with a concomitant increase in fluorescent quantum yield is consistent with the exposure of the fluorophore (ANS molecules or tryptophan side chains) to a more hydrophobic environment (Lakowicz, 1983). While this may result from a conformational change in the protein (exposing more

Table 3: Effect of Intermediate Concentrations of Denaturant on Fluorescence  $\lambda_{\max}$  in the Range of 310–400 nm for mIL-6, IAA-IL-6, IAM-IL-6, and DTT-IL-6 at pH 7.4 and 4.0<sup>a</sup>

protein	$\lambda_{\max}$ (nm)				
	pH 4.0		pH 7.4		
	1 M GdnHCl	2 M urea	1 M GdnHCl	2 M urea	
mIL-6	344	345	345	347	347
IAA-IL-6	345	333	345	335	345
IAM-IL-6	345	332	345	341	334
DTT-IL-6	335	332	335	333	334

<sup>a</sup> All protein concentrations were 40  $\mu\text{g/mL}$ . The excitation wavelength was 295 nm.

Table 4: Values of  $[D]_{50\%}$  for the GdnHCl-Induced Denaturation of the Intermediate States of Modified and Unmodified mIL-6 at pH 7.4, Monitored by Intrinsic Fluorescence Emission at 335 nm, Intrinsic  $\lambda_{\max}$  in the Range of 310–400 nm, Change in the CD Signal at 222 nm, and ANS  $\lambda_{\max}$  in the Range of 410–590 nm<sup>a</sup>

detection method	mIL-6	DTT-IL-6	IAA-IL-6	IAM-IL-6
intrinsic $F_{1335\text{ nm}}$	$2.1 \pm 0.1$	$2.5 \pm 0.01$	$2.1 \pm 0.03$	$2.3 \pm 0.02$
intrinsic $\lambda_{\max}$	$2.2 \pm 0.0$	$2.7 \pm 0.02$	$2.3 \pm 0.03$	$2.4 \pm 0.02$
CD <sub>222 nm</sub>	$2.8 \pm 0.1$	$3.5 \pm 0.2$	$2.5 \pm 0.1$	$2.9 \pm 0.1$
ANS $\lambda_{\max}$	$2.1 \pm 0.1$	$3.4 \pm 0.9$	$2.5 \pm 0.02$	$2.7 \pm 0.02$

<sup>a</sup>  $[D]_{50\%}$  was estimated by fitting data corresponding to the intermediate states and major unfolding phase to eq 1, where  $a = 0$ . Units are moles per liter; the tolerances shown are fitting errors.

hydrophobic surface area or burial of tryptophan residues), it may also result from protein aggregation. By examining the effect of protein concentration on the intrinsic fluorescence  $\lambda_{\max}$ , we have previously shown that mIL-6 unfolding intermediates aggregate (Ward et al., 1995). Here we look at the effect of protein concentration and the presence of 1 M GdnHCl and 2 M urea on the intrinsic fluorescence  $\lambda_{\max}$  of mIL-6 and its cysteine-modified derivatives. The intrinsic fluorescence  $\lambda_{\max}$  of mIL-6 is unaffected by protein concentrations of up to 1000  $\mu\text{g/mL}$  in the absence of denaturant at both pH 4.0 and 7.4 but exhibits a concentration-dependent blue shift of  $\lambda_{\max}$  at pH 7.4 in the presence of 1.5 M GdnHCl (Ward et al., 1995). At 40  $\mu\text{g/mL}$ , however, there is no significant change in  $\lambda_{\max}$  upon the addition of denaturant at either pH 4.0 or 7.4. This is consistent with decreased changes of intrinsic fluorescence properties in the unfolding of mIL-6 in this study (40  $\mu\text{g/mL}$ ) compared with those performed at 100  $\mu\text{g/mL}$  (Ward et al., 1995). In contrast, the cysteine-modified derivatives of mIL-6 show concentration-dependent blue-shifts of  $\lambda_{\max}$  at lower protein concentrations than were observed for the unfolding intermediates of mIL-6 (i.e., pH 7.4, 1.5 M GdnHCl; data for mIL-6 and IAM-IL-6 shown in Tables 2 and 3). DTT-IL-6 shows appreciable association under all conditions studied. At pH 4.0, IAM-IL-6 showed association effects in the presence of both 1 M GdnHCl and 2 M urea, while IAA-IL-6 association is only observed in the presence of 1 M GdnHCl. At pH 7.4, in the presence of 1 M GdnHCl, both IAA-IL-6 and IAM-IL-6 show association effects, while IAM-IL-6 additionally exhibits a small blue-shift of  $\lambda_{\max}$  even in the absence of denaturant and larger blue-shifts upon the addition of 2 M urea. Thus, a loose ranking of the tendency of mIL-6 and derivatives to self-associate is mIL-6 < IAA-IL-6 < IAM-IL-6  $\ll$  DDT-IL-6.

The ability of DTT-IL-6 to self-associate was also studied using a biosensor employing surface plasmon resonance (SPR) detection. DTT should reduce both the unbound and sensor surface-bound forms of mIL-6 to DTT-IL-6. The presence of 10 mM DTT caused unbound DTT-IL-6 (40  $\mu$ g/mL) to associate with sensor surface-bound DTT-IL-6, whereas no such association was apparent in the absence of DTT (data not shown). The results from that experiment cannot be directly compared in a quantitative manner with others in this study because very different buffer systems (e.g., HEPES/NaCl/EDTA/Tween-20 for biosensor experiments vs Tris-HCl for fluorescence and CD experiments) were used. However, these studies support the postulate that DTT-IL-6 exists in a highly aggregated state.

## DISCUSSION

IL-6 contains four cysteine residues, which are highly conserved over the known species of IL-6 (which at the time of writing includes 11 full and 1 partial sequence from 12 different species; Simpson et al., 1997) as well as the sequentially related granulocyte colony-stimulating factor (G-CSF; Hirano et al., 1986). These cysteine residues form two disulfide bonds which have been characterized for mouse IL-6 (Simpson et al., 1988a), human IL-6 (Clogston et al., 1989), and human G-CSF (Lu et al., 1989). From a homology model of mIL-6 (Hammacher et al., 1994) based on the X-ray-determined structure of G-CSF (Hill et al., 1993), the disulfide bonds Cys44–Cys50 and Cys73–Cys83 are positioned at nearly opposite faces of the molecule, forming loops which link the C-terminal section of the putative A helix and N-terminal section of the putative B helix to nearby regions of the long A/B loop. These disulfide bonds readily reform from a reduced and denatured state (Zhang et al., 1992). We anticipated, therefore, that these modifications to relatively solvent-exposed regions might provide enough disruption of structure to promote a partially folded conformation, without totally destroying the protein structure.

Previous studies have shown that eliminating both of the equivalent disulfide bonds in hIL-6 by either site-directed mutagenesis or S-alkylation of reduced hIL-6 virtually eliminates activity while retaining at least partial structure (Snouwaert et al., 1991; Rock et al., 1994). In agreement with this, the activities of the reduced and alkylated forms of mIL-6 show a much reduced activity (200–500-fold) over mIL-6 (Figure 1A). Under normal circumstances, IL-6 binds first to its specific receptor (IL-6R), and this binary complex further binds to a signal-transducing protein, gp130 (Yamasaki et al., 1988). The loss of activity here is due in the first instance to the inability of IAA-IL-6 and IAM-IL-6 to bind to IL-6R, as shown in the binding assay (Figure 1B). For hIL-6, the breaking of the Cys44–Cys50 disulfide bond produced only a small loss of activity, while the breaking of the Cys73–Cys83 disulfide bond (or both bonds) caused the major reduction of activity (Snouwaert et al., 1991; Rock et al., 1994). We were unable to differentially reduce and alkylate mIL-6, so at this stage, we are unable to determine if the Cys73–Cys83 bond is also more important for biological activity than Cys44–Cys50 in mIL-6.

While the activities of IAA-IL-6 and IAM-IL-6 are similar, their stabilities estimated by urea denaturation at pH 4.0 (Figure 5, Table 1) differ in that IAA-IL-6 has a thermody-

namic stability equivalent to that of mIL-6, whereas IAM-IL-6 is significantly less stable. These differences in stability may account for the differential activity between the two modified proteins but do not account for loss of activity compared with that of mIL-6. To do this, we must consider their conformational properties, and whether the disulfide-disrupted derivatives of mIL-6 have molten globule-like properties, as have been reported for the biologically active but single-disulfide variant of hIL-6 under acidic conditions (De Filippis et al., 1996).

Because molten globule states have a tendency to aggregate, they can be difficult to characterize (Kim & Baldwin, 1990). It is difficult, even using a variety of monitoring techniques, to distinguish clearly between aggregated molten globule and aggregated non-molten globule (e.g., denatured or misfolded) states. However, there are several properties which in combination are used to characterize the molten globule state, including the presence of secondary structure in the absence of tertiary structure, an increased tendency to bind ANS, and an increased hydrodynamic volume.

There is a high degree of  $\alpha$ -helical content, as determined by far-UV CD, at both pH 4.0 and 7.4 for mIL-6, IAA-IL-6, and IAM-IL-6. In contrast, near-UV CD shows that mIL-6 retains a high degree of tertiary structure at both pH 4.0 and 7.4 (unlike the single-disulfide hIL-6 variant, which shows a partial loss of tertiary structure at pH 4.0; De Filippis et al., 1996). IAA-IL-6 and IAM-IL-6 have a diminished near-UV signal, but native-like spectrum at pH 7.4, which is further reduced at pH 4.0. These studies suggest that both IAA-IL-6 and IAM-IL-6 have a native-like fold in terms of secondary structure; however, the tertiary structure is much looser in the alkylated derivatives, with the aromatic residues being in less constrained environments. DTT-IL-6, however, has a much reduced far-UV CD signal at 222 nm at pH 7.4, and the change of the  $\Theta_{222\text{nm}}/\Theta_{208\text{nm}}$  ratio at pH 7.4 from  $<1$  for mIL-6, IAA-IL-6, and IAM-IL-6 to  $>1$  for DTT-IL-6 implies that the reduced protein has lost something of the typical four- $\alpha$ -helix bundle structure, either as a direct result of aggregation or by a further loosening of the overall structure. Unfortunately, we cannot obtain near-UV CD spectra for DTT-IL-6 to resolve this issue.

In terms of ANS binding, all proteins show an 8–15-fold increase of apparent ANS binding at pH 4.0 compared with that at pH 7.4. This appears to be due more to effects of the overall charge of mIL-6 rather than pH-induced conformational changes as, for example, mIL-6 has an 8-fold increase in ANS fluorescence quantum yield at pH 4.0 over pH 7.4, but there appears to be little, if any, structural differences as determined by CD. At both pH 4.0 and 7.4, DTT-IL-6 and, to a lesser extent, IAM-IL-6 have an enhanced ANS fluorescence over mIL-6 which seemed to correlate closely with an increased tendency to aggregate. The low levels of ANS binding to IAA-IL-6 relative to mIL-6 and IAM-IL-6 also appear to be due to charge effects.

At the low protein concentrations mainly used for these conformational and folding studies (40–50  $\mu$ g/mL), the intrinsic fluorescence of IAA-IL-6 and IAM-IL-6 is close to that of mIL-6. When the protein concentration is increased, however, a blue-shift of  $\lambda_{\text{max}}$  suggests that IAA-IL-6 and IAM-IL-6 are prone to aggregate at concentrations where mIL-6 does not. This is particularly so at pH 7.4, where IAM-IL-6 shows a blue shift of  $\lambda_{\text{max}}$  at the lowest protein concentration studied and under conditions where



mIL-6 has a net neutral charge (Ward et al., 1995). Thus, it appears that the S-alkylated derivatives have loosely folded structures at both pH values and a higher tendency to aggregate under conditions where the protein has a low net charge. Similar pH dependencies of aggregated folding intermediates were observed for mIL-6 where a low net charge on the protein at pH 7.4 favored aggregation. Aggregation of mIL-6 folding intermediates was also induced by increasing salt concentrations which presumably shields the charge on the protein (Ward et al., 1995; Matthews et al., 1996). In contrast, DTT-IL-6 shows enhanced intrinsic fluorescence and blue-shifted  $\lambda_{\text{max}}$ , indicating that it is aggregated under all conditions studied.

When monitored by SEC, proteins which unfold in a two-state manner are usually characterized by the disappearance of one peak which corresponds to the native protein and the emergence of a second peak which corresponds to the denatured protein at increasing concentrations of denaturant (Uversky, 1993). Those proteins which unfold via intermediates (including molten globule states) tend to show a shift in retention volume with the broader peaks indicative of mixtures of intermediate forms (Uversky, 1993). Our data resemble those of proteins which unfold via such intermediates, with broad peaks in the transition region.

At pH 7.4, the aggregated unfolding intermediates of all four proteins unfold in a cooperative manner as detected by intrinsic and extrinsic fluorescence and CD. The data from these unfolding transitions have been analyzed using eq 1 (Table 4) which has shown that, other than the unfolding of DTT-IL-6 monitored by far-UV CD and ANS fluorescence, most of the values of  $[D]_{50\%}$  occur over a fairly small range of denaturant concentrations (2.1–2.9 M GdnHCl), the order of which also corresponds to their tendency to aggregate (highest  $[D]_{50\%}$  = highest tendency to aggregate). The differences in  $[D]_{50\%}$  may reflect a reduced accessibility to solvent of the aggregated forms, while their similarities are probably a measure of the thermostability of the  $\alpha$ -helices and nonspecific hydrophobic interactions which may maintain the compact nature of the intermediates (Griko et al., 1994; Khurana & Udgaonkar, 1994). In this sense, the unfolding intermediates in this study resemble some of the *de novo*-designed proteins which have a high degree of secondary structure, imperfectly packed hydrophobic cores, and relatively high thermostability (Hecht et al., 1990; Beauregard et al., 1991; Tankake et al., 1994; Quinn et al., 1994). The conformational differences between DTT-IL-6 and the S-alkylated derivatives of mIL-6 may be caused by the alkylating groups of IAA-IL-6 and IAM-IL-6 having a decreased entropy and potentially higher degrees of structure.

Both mIL-6 and the single-disulfide variant of hIL-6 (De Filippis et al., 1996) show enhanced ANS binding and high secondary structure content at pH 4.0. However, mIL-6 does not show the reduction of tertiary structure which is observed for the hIL-6 variant, suggesting that fewer conformational changes are induced at lower pH for the two-disulfide murine molecule. Disruption of both disulfide bonds in mIL-6 does not necessarily affect thermodynamic stability but appears to induce partially unfolded conformations which have some molten globule-like properties. This suggests that the disulfide bonds of mIL-6 help to maintain conformational integrity.

The similarity of mIL-6 aggregates formed at very high protein concentrations (10–20 mg/mL; Morton et al., 1995)

and mIL-6 equilibrium unfolding intermediates (Ward et al., 1995) imply that aggregates accumulate by the association of partially unfolded intermediates, which are present in higher levels at higher protein concentrations, even in the absence of denaturant. This formation of mIL-6 aggregates is markedly increased at higher, but not extreme, temperatures (up to 40 °C; Morton et al., 1995), suggesting that partially unfolded intermediates are readily formed at physiological temperatures and may exist at relatively high concentrations in equilibrium with the fully folded protein. Whether this is the case, and whether higher-temperature molten globule conformations do confer a protection toward proteolysis similar to that observed for the A-state of the hIL-6 variant (De Filippis et al., 1996), is yet to be determined.

In summary, the reduction of the two disulfide bonds in mIL-6 causes the protein to take up a partially unfolded and highly aggregated conformation. Alkylation of these disulfide bonds significantly reduces the biological activity of mIL-6 and causes the protein to take up partially unfolded conformations with some molten globule-like properties, including a high degree of secondary structure, but low levels of tertiary structure. All of these partially unfolded conformational states have a high propensity to aggregate, the degree of which is dependent on the type of modification (DTT  $\gg$  IAM > IAA). The physicochemical properties of these aggregated conformations closely resemble those of the equilibrium unfolding intermediates of wild-type recombinant mIL-6.

## REFERENCES

- Bazan, J. F. (1990) *Immunol. Today* 11, 350–354.
- Beauregard, M., Goraj, K., Goffin, V., Heremans, K., Goormaghtigh, E., Ruysschaert, J. M., & Martial, J. A. (1991) *Protein Eng.* 4, 745–749.
- Breton, J., La Fiura, A., Bertolero, F., Orsini, G., Valsassina, B., Ziliotto, R., De Filippis, V., Polverino de Laureto, P., & Fontana, A. (1995) *Eur. J. Biochem.* 227, 573–581.
- Clarke, J., & Fersht, A. R. (1993) *Biochemistry* 32, 4322–4329.
- Clogston, C. I., Boone, T. C., Crandell, C., Mendiaz, E. A., & Lu, H. S. (1989) *Arch. Biochem. Biophys.* 272, 144–151.
- Cooper, T. M., & Woody, R. W. (1990) *Biopolymers* 30, 657–676.
- Creighton, T. E., & Ewbank, J. J. (1994) *Biochemistry* 33, 1534–1538.
- De Filippis, V., Polverino de Laureto, P., Toniutti, N., & Fontana, A. (1996) *Biochemistry* 35, 11503–11511.
- Dolgikh, D. A., Gilmanshin, R. I., Braznikov, E. V., Bychova, V. E., Semisotnov, G. V., Venyaminov, S. Y., & Ptitsyn, O. B. (1981) *FEBS Lett.* 136, 311–315.
- Flynn, G. C., Beckers, C. J., Baases, W. A., & Dahlquist, F. W. (1993) *Proc. Natl. Acad. Sci. U.S.A.* 90, 10826–10830.
- Glazer, A. N., Delange, R. J., & Sigman, D. S. (1975) in *Chemical Modification of Proteins: Selected Methods and Analytical Procedures* (Work, T. S., & Work, E., Eds.) North-Holland/American Elsevier, Oxford and New York.
- Goto, Y., & Fink, A. L. (1989) *Biochemistry* 28, 945–952.
- Griko, Y. V., Freire, E., & Privalov, P. L. (1994) *Biochemistry* 33, 1889–1899.
- Hagihara, Y., Aimoto, S., Fink, A. L., & Goto, Y. (1993) *J. Mol. Biol.* 231, 180–184.
- Hammacher, A., Ward, L. D., Weinstock, J., Treutlein, H., Yasukawa, K., & Simpson, R. J. (1994) *Protein Sci.* 3, 2280–2293.
- Hayer-Hartl, M. K., Ewbank, J. J., Creighton, T. E., & Hartl, F. U. (1994) *EMBO J.* 13, 3192–3202.
- Hecht, M. H., Richardson, J. S., Richardson, D. C., & Ogden, R. C. (1990) *Science* 249, 884–891.

- Hill, C. P., Osslund, T. D., & Eisenberg, D. (1993) *Proc. Natl. Acad. Sci. U.S.A.* 90, 5167–5171.
- Hirano, T. (1994) in *The Cytokine Handbook* (Thompson, A., Ed.) 2nd ed., pp 145–168, Academic Press, San Diego.
- Hirano, T., Yasakuwa, K., Harada, H., Taga, T., Watanabe, Y., Matsuda, T., Kashiwamura, S.-I., Nakajima, K., Koyama, K., Iwamatsu, A., Tsunasawa, S., Sakiyama, F., Matsui, H., Takahara, Y., Taniguchi, T., & Kishimoto, T. (1986) *Nature* 324, 73–76.
- Khurana, R., & Udgaonkar, J. B. (1994) *Biochemistry* 33, 106–115.
- Kim, P. S., & Baldwin, R. L. (1990) *Annu. Rev. Biochem.* 59, 631–660.
- Klein, B., Zhang, X.-G., Lu, Z.-Y., & Bataille, R. (1995) *Blood* 85, 863–872.
- Kreimer, D. I., Szosenfogel, R., Goldfarb, D., Silman, I., & Weiner, L. (1994) *Proc. Natl. Acad. Sci. U.S.A.* 91, 12145–12149.
- Kuwajima, K. (1989) *Proteins: Struct., Funct., Genet.* 6, 87–103.
- Kuwajima, K., Ikeguchi, M., Sugawar, T., Hiraoka, Y., & Sugai, S. (1990) *Biochemistry* 29, 8240–8249.
- Lakowicz, J. R. (1983) in *Principles of Fluorescence Spectroscopy*, Plenum Press, New York.
- Landegren, U. (1984) *J. Immunol. Methods* 67, 379–388.
- Lu, H. S., Boone, T. C., Souza, L. M., & Lai, P. H. (1989) *Arch. Biochem. Biophys.* 268, 81–92.
- Matthews, J. M., Ward, L. D., Zhang, J. G., & Simpson, R. J. (1996) *Techniques Protein Chem.* 7, 449–457.
- Morton, C. J., Bai, H., Zhang, J.-G., Hammacher, A., Norton, R. S., Simpson, R. J., & Mabbitt, B. C. (1995) *Biochim. Biophys. Acta* 1249, 189–203.
- Nakajima, K., Martinez-Maza, O., Hirano, T., Breen, E. C., Nishanian, P. G., Salazar-Gonzales, J. F., Fahey, J. L., & Kishimoto, T. (1989) *J. Immunol.* 142, 144–147.
- Narazaki, M., & Kishimoto, T. (1994) In *Guidebook to cytokines and their receptors* (Nicola, N. A., Ed.) pp 1–7, Oxford University Press: New York.
- Nishimura, C., Watanabe, A., Gouda, H., Shimadada, I., & Arata, Y. (1996) *Biochemistry* 35, 273–281.
- Peng, X., Jonas, J., & Silva, J. L. (1994) *Biochemistry* 33, 8323–8329.
- Ptitsyn, O. B. (1987) *J. Protein Chem.* 6, 272–293.
- Ptitsyn, O. B. (1992) in *Protein Folding* (Creighton, T. E., Ed.) pp 243–300, W. H. Freeman & Co., New York.
- Ptitsyn, O. B. (1995) *Adv. Protein Chem.* 47, 83–229.
- Quinn, T. P., Tweedy, N. B., Williams, R. W., Richardson, J. S., & Richardson, D. C. (1994) *Proc. Natl. Acad. Sci. U.S.A.* 91, 8747–8751.
- Rock, F. L., Li, X., Chong, P., Ida, N., & Klein, M. (1994) *Biochemistry* 33, 5146–5154.
- Santoro, M. M., & Bolen, D. W. (1988) *Biochemistry* 27, 8063–8068.
- Silver, I. A., Murrills, R. J., & Etherington, D. J. (1988) *Exp. Cell. Res.* 175, 266–267.
- Simpson, R. J., Moritz, R. L., Nice, E. C., Grego, B., Yoshizaki, F., Sugimura, Y., Freeman, H., & Murata, M. (1986) *Eur. J. Biochem.* 157, 497–506.
- Simpson, R. J., Moritz, R. L., van Roost, E., & van Snick, J. (1988a) *Biochem. Biophys. Res. Commun.* 157, 364–372.
- Simpson, R. J., Moritz, R. L., Rubira, M. R., & van Snick, J. (1988b) *Eur. J. Biochem.* 176, 187–197.
- Simpson, R. J., Hammacher, A., Smith, D. K., Matthews, J. M., & Ward, L. D. (1997) *Protein Sci.* (in press).
- Snouwaert, J. N., Leebeck, F. W. G., & Fowlkes, D. M. (1991) *J. Biol. Chem.* 266, 23097–23102.
- Tankake, T., Kimura, H., Hayashi, M., Fujiyoshi, Y., Fukuhara, K., & Nakamura, H. (1994) *Protein Sci.* 3, 419–427.
- Thomas, P. J., Qu, B.-H., & Pederson, P. L. (1995) *Trends Biochem. Sci.* 20, 456–459.
- Uversky, V. N. (1993) *Biochemistry* 32, 13288–13298.
- van Snick, J., Cayphas, S., Vink, A., Uyttenhove, C., Coulie, P., Rubira, M. R., & Simpson, R. J. (1986) *Proc. Natl. Acad. Sci. U.S.A.* 83, 9679–9683.
- Ward, L. D., Hammacher, A., Zhang, J.-G., Weinstock, J., Yasukawa, K., Morton, C. J., Norton, R. S., & Simpson, R. J. (1993) *Protein Sci.* 2, 1472–1481.
- Ward, L. D., Matthews, J. M., Zhang, J.-G., & Simpson, R. J. (1995) *Biochemistry* 34, 11652–11659.
- Wicar, S., Mulkerrin, M. G., Bathory, G., Khundkar, L. H., & Karger, B. L. (1994) *Anal. Chem.* 66, 3908–3915.
- Yamasaki, K., Taga, T., Hirata, Y., Yawata, H., Kawanishi, Y., Seed, B., Taniguchi, T., Hirano, T., & Kishimoto, T. (1988) *Science* 241, 825–828.
- Yang, J. T., Wu, C.-S. C., & Martinez, H. M. (1986) *Methods Enzymol.* 130, 208–269.
- Zhang, J.-G., Moritz, R. M., Reid, G. E., Ward, L. W., & Simpson, R. J. (1992) *Eur. J. Biochem.* 207, 903–913.

BI962164R